DEEP BRAIN STIMULATION

Optimized temporal pattern of brain stimulation designed by computational evolution

David T. Brocker,[1] Brandon D. Swan,[1] Rosa Q. So,[1] Dennis A. Turner,[2,3] Robert E. Gross,[4,5] Warren M. Grill[1,2]*

Brain stimulation is a promising therapy for several neurological disorders, including Parkinson's disease. Stimulation parameters are selected empirically and are limited to the frequency and intensity of stimulation. We varied the temporal pattern of deep brain stimulation to ameliorate symptoms in a parkinsonian animal model and in humans with Parkinson's disease. We used model-based computational evolution to optimize the stimulation pattern. The optimized pattern produced symptom relief comparable to that from standard high-frequency stimulation (a constant rate of 130 or 185 Hz) and outperformed frequency-matched standard stimulation in a parkinsonian rat model and in patients. Both optimized and standard high-frequency stimulation suppressed abnormal oscillatory activity in the basal ganglia of rats and humans. The results illustrate the utility of model-based computational evolution of temporal patterns to increase the efficiency of brain stimulation in treating Parkinson's disease and thereby reduce the energy required for successful treatment below that of current brain stimulation paradigms.

INTRODUCTION

Parkinson's disease (PD) is a progressive, neurodegenerative disease characterized by motor symptoms that include bradykinesia, resting tremor, postural instability, and rigidity (*1*, *2*). Although dopamine replacement therapy treats the symptoms of PD, its long-term use is complicated by the requirement for higher and more frequent dosing, motor fluctuations, and dyskinesias (*3*). Deep brain stimulation (DBS) is an effective and adjustable surgical treatment for advanced PD (*4*, *5*) that improves motor symptoms and quality of life and reduces motor fluctuations (*6*). However, this therapy has not been optimized, and there have been few improvements in DBS since its introduction.

The stimulation parameters used for DBS are determined empirically and consist of short-duration (60- to 180-μs), high-frequency (typically 130- to 185-Hz) pulses of electrical stimulation to ameliorate symptoms (*7*–*9*). The efficacy of DBS is strongly dependent on the frequency of stimulation: low-frequency stimulation (<50 Hz) is ineffective or exacerbates symptoms, whereas high-frequency stimulation produces symptomatic benefit. Unfortunately, high stimulation frequencies also cause stronger side effects (*10*, *11*) and consume more energy (*12*) than low-frequency stimulation, leading to frequent surgical replacement of battery-powered, implanted pulse generators (IPGs) (*13*). IPG replacement surgeries are expensive and carry risks, including infection and misprogramming (*14*).

Current DBS systems deliver a regular temporal pattern of stimulation; interpulse intervals do not vary as a function of time. Irregular temporal patterns of stimulation have been used in animal (*15*–*17*) and human studies (*18*–*22*) to probe DBS mechanisms. Random patterns of DBS, even when delivered at a high average frequency, are not effective in ameliorating parkinsonian symptoms in rats (*17*), tremor in persons with essential tremor (*21*, *22*), or bradykinesia in patients with PD (*18*). These results indicate that the effects of DBS on symptoms are strongly dependent on the temporal pattern of stimulation and motivated our current study in which we sought to design a temporal stimulation pattern for DBS that would be more efficient than conventional high-frequency DBS.

[1]Department of Biomedical Engineering, Duke University, Durham, NC 27708, USA. [2]Department of Neurobiology, Duke University Medical Center, Durham, NC 27710, USA. [3]Department of Neurosurgery, Duke University Medical Center, Durham, NC 27710, USA. [4]Departments of Neurosurgery and Neurology, Emory University, Atlanta, GA 30322, USA. [5]Coulter Department of Biomedical Engineering, Georgia Institute of Technology, Atlanta, GA 30332, USA.
*Corresponding author. Email: warren.grill@duke.edu

RESULTS

Design of optimized temporal pattern of stimulation with computational evolution

We used model-based computational evolution to design an optimized temporal pattern of stimulation that reduced the average stimulation frequency of DBS and preserved efficacy (thereby decreasing the energy requirement for stimulation and consequent risks associated with frequent IPG replacements). A model of the basal ganglia was coupled with a genetic algorithm (GA) and was used in the design of optimized stimulation pattern. GAs are well suited to this problem, where there is a highly complex, nonlinear relationship between the input (stimulus pattern) and output (neural activity). The GA operates analogously to evolution through natural selection, in which the "organisms" are the temporal patterns of DBS. The GA was used to design a stimulation pattern that minimized average stimulation frequency and error index (EI), a model-based proxy for symptoms (Fig. 1A). The EI is a measure of the fidelity of information transmission through the thalamus under modulation by the output of the basal ganglia (*23*) and was used here as a proxy for parkinsonian bradykinesia (Fig. 1B) (*18*). The fitness of each stimulation pattern was evaluated with a cost function that incentivized reducing both EI and the average stimulation frequency. Patterns with greater fitness were more likely to pass their genes (pattern characteristics) to the next generation of patterns (Fig. 1, C and D). The cost of the best stimulation pattern in each generation declined monotonically across generations, whereas the median cost across the population in each generation declined more slowly (Fig. 1E). The resulting optimal pattern had an average frequency of 45 Hz and reduced the EI in the model by almost 98% relative to a 45-Hz, constant-frequency stimulation (Fig. 1F).

Efficacy of optimized GA pattern of stimulation in hemiparkinsonian rats

The optimized pattern of DBS (GA) was compared to DBS off (baseline), 45-Hz DBS, and 130-Hz DBS in hemiparkinsonian rats by using

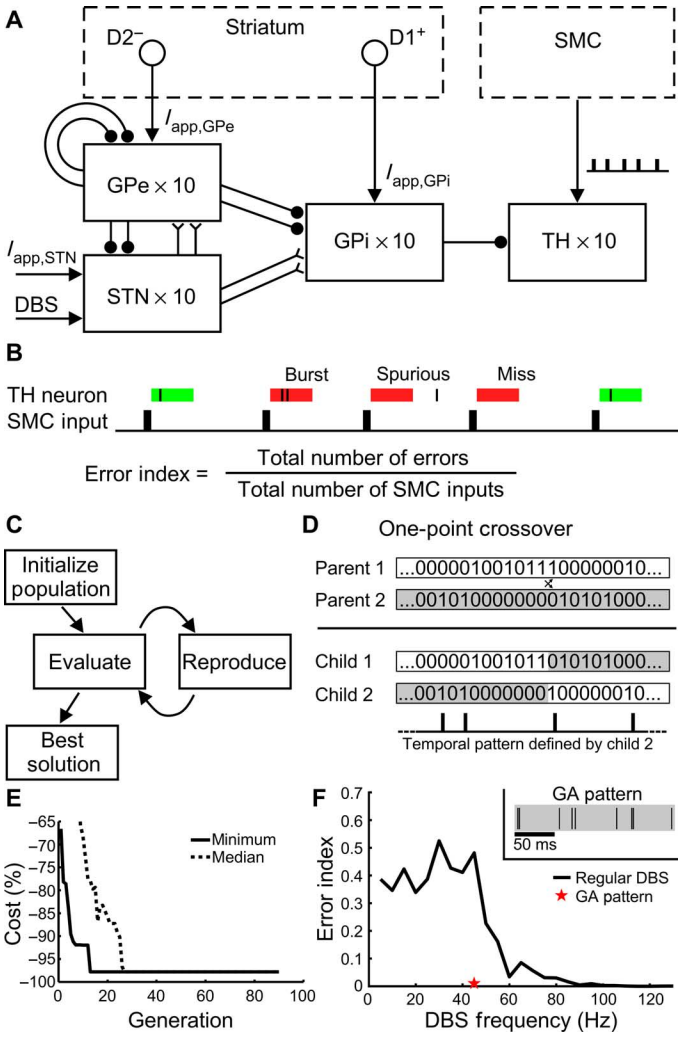

Fig. 1. Model-based design by computational evolution of an optimized temporal pattern of DBS. (**A**) Computational model of the parkinsonian basal ganglia that included the external globus pallidus (GPe), subthalamic nucleus (STN), internal GP (GPi), thalamus (TH), and an input action potential train from the sensorimotor cortex (SMC). Applied currents (→) representing inputs to GPe, GPi, and STN were modeled ($I_{app,GPe}$, $I_{app,GPi}$, and $I_{app,STN}$); GPe primarily receives inputs from striatal neurons expressing inhibitory D2-type receptors ($D2^-$), whereas GPi primarily receives inputs from striatal neurons expressing excitatory D1-type receptors ($D1^+$). Excitatory and inhibitory synapses are depicted using forked (Y) and circular (●) terminations. (**B**) The EI, a measure of the fidelity of thalamic neuron response to SMC input. If a thalamic neuron did not fire an action potential within 25 ms of an SMC input, an error occurred. There were three types of errors: misses, bursts, and spurious. EI was defined as the total number of errors divided by the total number of SMC inputs. (**C**) Diagram of the GA. A random population of stimulation patterns was initialized. Subsequent generations of patterns were created by using principles from biological evolution and were evaluated according to the cost function. After convergence, the pattern with the lowest cost (GA) was selected to be tested in the hemiparkinsonian rats and human patients. (**D**) Representation of stimulation patterns. Defined by binary strings, new patterns were created by one-point crossover. (**E**) Trajectory of convergence to the GA pattern of stimulation during successive generations of modeling. (**F**) EI of standard (black line) and the optimized GA (red star) stimulation pattern. Inset: A 200-ms segment of the repeating GA pattern of stimulation.

two well-established measures of parkinsonian symptoms that exhibit DBS frequency-dependent effects that parallel those observed in clinical studies (*24*): the bar test to assess akinesia (Fig. 2A) and methamphetamine-induced circling to assess locomotor behavior (Fig. 2B).

There was a significant effect of stimulation condition on time on the bar, and all patterns of stimulation reduced time on the bar compared to baseline. Both 130 Hz and GA significantly reduced time on the bar compared to 45 Hz (Fig. 2C). Similarly, there was a significant effect of stimulation condition on circling rate, and all patterns of DBS reduced circling rate compared to baseline. High-frequency (130-Hz) DBS reduced circling rate more completely than did 45 Hz or GA. Although in humans with PD <50-Hz DBS is ineffective and 130 to 185 Hz is used for treatment, in 6-hydroxydopamine (6-OHDA)–lesioned rats DBS at 30 to 75 Hz is at least partially effective at treating parkinsonian symptoms including methamphetamine-induced circling (*24*, *25*), akinesia (*24*), and reduced open-field mobility (*26*). Thus, in parkinsonian rats, the optimized GA stimulation pattern performed better than the partially effective standard 45 Hz, although 130-Hz DBS performed better than either. There was no effect of stimulation condition on normalized distance traveled (fig. S1); the results from this control indicated that the reductions in circling rate achieved by DBS (Fig. 2D) did not simply reflect decreases in overall movement or activity but rather demonstrated a resolution of the pathological circling behavior (*25*).

Efficacy of optimized pattern of stimulation in subjects with PD

We quantified unilateral motor symptoms—either bradykinesia or tremor—on the more affected side in subjects with STN DBS for PD (Table 1) undergoing IPG replacement surgery during DBS off (baseline), temporally regular 185-Hz DBS (185 Hz), temporally regular 45-Hz DBS (45 Hz), and the optimized GA pattern with an average frequency of 45 Hz (GA) (table S1).

We tested bradykinesia-dominant PD subjects (n = 4) with an alternating finger-tapping task (*27*), a quantitative outcome measure strongly correlated with clinical measures of bradykinesia (Fig. 3, A and B) (*20*, *27*). There was a significant effect of stimulation condition on the rate (fig. S2) and regularity (Fig. 3C) of finger tapping. Both GA and 185 Hz significantly improved both the rate and regularity of finger tapping compared to baseline, but 45 Hz only improved tapping rate. Tapping variability was not different between GA and 185 Hz, and both were lower than 45 Hz.

We exploited the correlation between the regularity of finger tapping and Unified Parkinson's Disease Rating Scale (UPDRS) part III motor examination subscores (*20*, *27*) to estimate the clinical impact of the different patterns of stimulation. The finger-tapping data suggested that 185 Hz reduced UPDRS motor scores by nearly 34 points on average compared to baseline (Fig. 3D), consistent with previously described effects of DBS (*28*), whereas GA was predicted to reduce UPDRS motor scores by 31 points. Both GA and 185 Hz were predicted to reduce UPDRS motor scores by over 12 points more on average than 45 Hz.

We quantified unilateral tremor in tremor-dominant PD subjects (n = 4) using an accelerometer attached to the dorsum of the hand (Fig. 4). There was a significant effect of DBS pattern on tremor (Fig. 4C). Tremor was decreased significantly compared to baseline by GA and 185 Hz. However, 45 Hz did not alter tremor relative to baseline. Furthermore, GA and 185 Hz both significantly decreased tremor compared to 45 Hz.

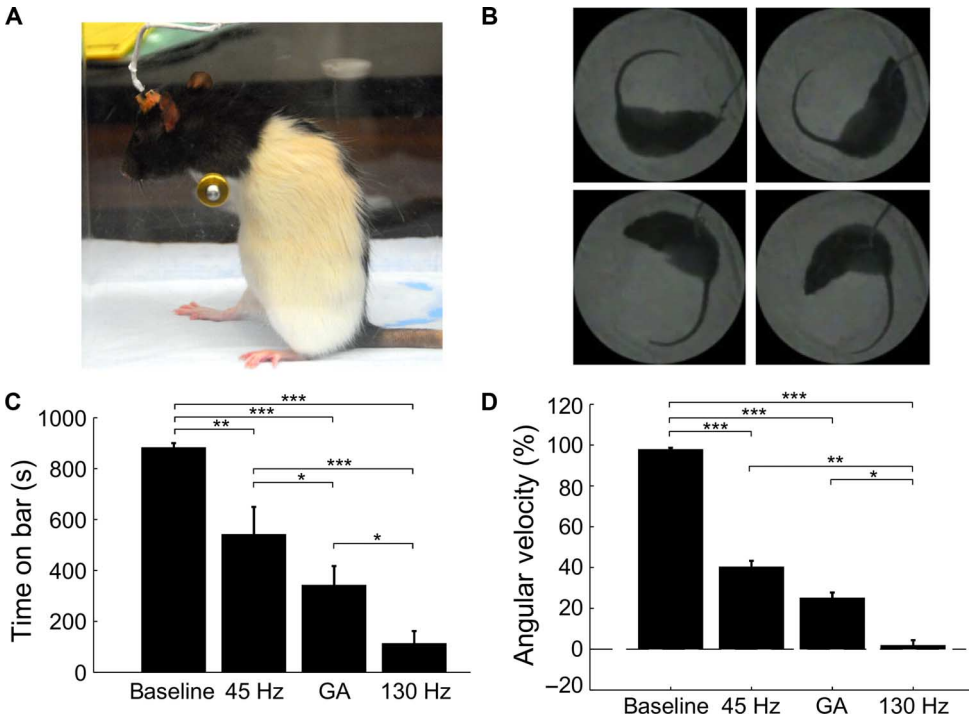

Fig. 2. Effects of temporal patterns of STN DBS on motor symptoms in hemiparkinsonian rats. Systems were evaluated using the bar test (**A**) and methamphetamine-induced circling (**B**). (**C**) Total time (means ± SEM) spent on the bar in all three stimulation conditions in the bar test (n = 9). Rats were akinetic and were unable to dismount from the bar during baseline, but DBS patterns differentially rescued akinesia. (**D**) Normalized circling rate (means ± SEM) across stimulation conditions (n = 13). The pathological ipsiversive circling rate was differentially reduced by the DBS patterns. Repeated-measures analysis of variance (RM-ANOVA) revealed a significant effect of stimulation condition on time on the bar ($P < 0.0001$) and normalized angular velocity ($P < 0.0001$). Fisher's protected least significant difference (PLSD) test was used to perform post hoc comparisons between stimulation conditions (*$P < 0.05$; **$P < 0.001$; ***$P < 0.0001$).

We used the logarithmic relationship (*29*) between tremor amplitude and a clinical tremor rating scale [TRS; 0 (no tremor) to 4 (severe tremor)] to estimate the clinical and functional impact of the patterns of DBS on tremor. The no-stimulation and 45-Hz conditions reduced the estimated TRS score by less than one point, whereas GA reduced the estimated TRS score by about two points, and 185 Hz eliminated tremor altogether (Fig. 4D). These data indicate that 185 Hz effectively suppressed tremor of all magnitudes, whereas GA suppressed completely only less severe tremor. GA DBS completely suppressed tremor in two tremor-dominant PD subjects effectively with a mean baseline tremor power of 61.5 m^2/s^4 but did not completely suppress tremor in two subjects with a mean baseline tremor power of 153 m^2/s^4.

Suppression of low-frequency oscillations

We hypothesized that the efficacy of temporal patterns of brain stimulation may be related to the suppression of the low-frequency oscillatory neural activity that is prevalent in PD (*30*) and in animal models of PD (*24*). Hemiparkinsonian rats exhibit exaggerated 7- to 10-Hz oscillations that are suppressed

Table 1. Subject information. M, male; F, female; AMP, amplitude; PW, pulse width; FREQ, frequency.

	Subject	Age/sex	Hemisphere/target tested	Electrode contacts*,†	AMP (V)†	PW (μs)	FREQ (Hz)	PD medications 12 hours before surgery
Bradykinesia	B1	55/M	Right/STN	$1^-/2^-/0^+$	3.9	60	185	None
	B2	59/M	Right/STN	$0^-/1^-/2^+$	3.5	60	185	None
	B3	69/F	Left/STN	$1^-/2^-/3^+$ [$1^-/2^-/C^+$]	2.6	60	185	10 mg of carbidopa 100 mg of levodopa
	B4	64/M	Right/STN	$1^-/2^-/3^+$ [$1^-/2^-/3^-/C^+$]	4.0 [1.9]	60	185	25 mg of carbidopa 250 mg of levodopa
Tremor	T1	69/M	Right/STN	$1^-/2^-/3^-/0^+$ [$1^-/2^-/3^-/C^+$]	3.5 [3.8]	90	135	None
	T2	66/M	Right/STN	$2^-/3^+$ [$2^-/C^+$]	2.2 [3.3]	60	130	None
	T3	66/M	Right/STN	$1^-/2^-/3^+$ [$1^-/2^-/C^+$]	3.2	60	180	None
	T4	59/F	Left/STN	$1^-/2^-/3^+$	2.5	90	180	None

*Quadripolar DBS electrode contacts are numbered 0 to 3, with 0 as most distal and 3 as most proximal. Contact polarity denoted by "+" (cathode) and "−" (anode). C^+ indicates that the IPG case was used as the anode (current return). †Experimental stimulation parameters are shown. Clinical settings different from the experimental settings are shown in brackets.

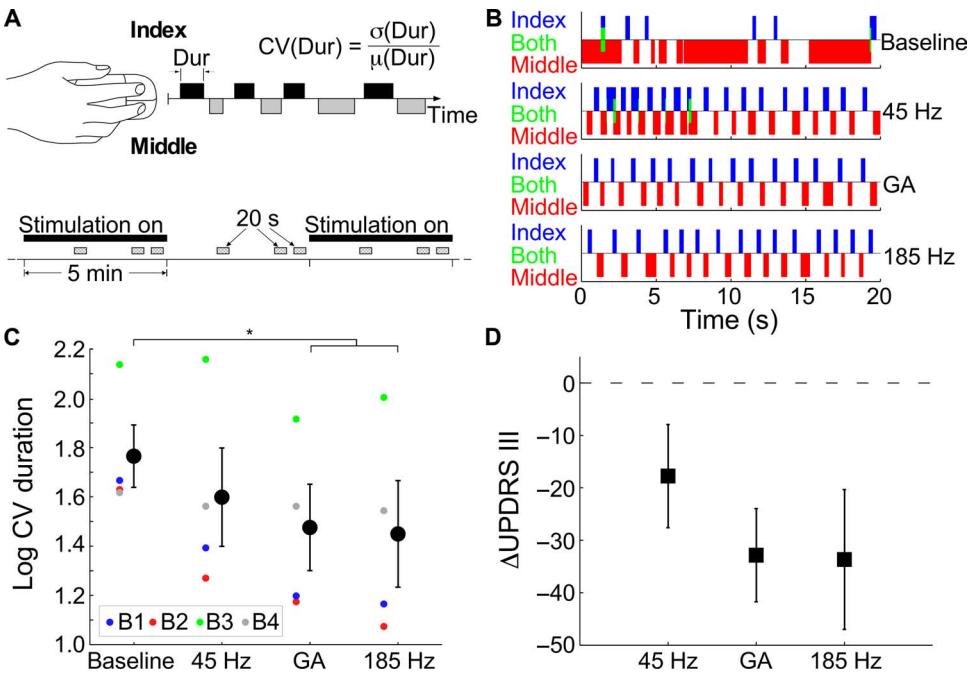

Fig. 3. Effects of temporal patterns of STN DBS on bradykinesia in persons with PD. (**A**) Diagram of data collection (top) and stimulation schedule (bottom) for evaluation of bradykinesia in PD subjects by using a finger-tapping task. Stimulation patterns were applied during the intraoperative experiment with 5-min on-off intervals, and finger-tapping data were collected for 20 s thrice during each 5-min epoch (crosshatched rectangles). The coefficient of variation (CV) of index finger tap durations (Dur) was calculated as the SD (σ) divided by the mean (μ) of the tap durations. (**B**) Data from subject B1 across the four experimental conditions. (**C**) Coefficient of variation for index finger tap durations (log-transformed) (means ± SEM) across stimulation conditions. RM-ANOVA revealed a significant effect of stimulation condition on regularity of finger tapping ($P = 0.01$; $n = 4$), and Fisher's PLSD test was used to perform post hoc comparisons between stimulation conditions (*$P < 0.05$). GA and 185-Hz DBS significantly improved performance in the finger-tapping task relative to baseline ($P = 0.006$ and $P = 0.004$, respectively). Tapping variability was lower for the GA and 185-Hz DBS conditions compared to the 45-Hz DBS condition, but the differences were not statistically significant ($P = 0.17$ and $P = 0.10$, respectively). Individual colored symbols represent individual participants. (**D**) Changes in UPDRS III scores (means ± SEM) from baseline for various stimulation patterns predicted from the finger-tapping task data.

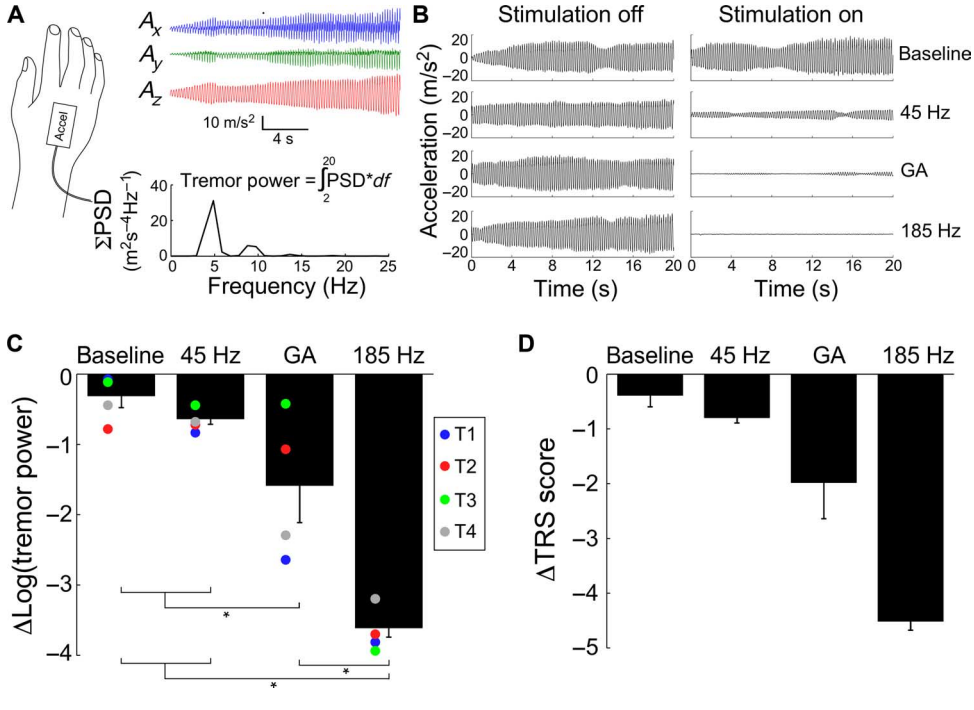

Fig. 4. Effects of temporal patterns of STN DBS on tremor in persons with PD. (**A**) Tremor was quantified in subjects with tremor-dominant PD by attaching an accelerometer to the dorsum of the hand. The power spectral density (PSD) was estimated and summed across the three orthogonal accelerometer axes (A_x, A_y, and A_z), and tremor power (m^2/s^4) was calculated by integrating the summed PSD (ΣPSD) with respect to frequency (*df*) in the 2- to 20-Hz range. (**B**) Tremor data from subject T1 across the four experimental conditions. (**C**) Changes in log-transformed tremor power (2 to 20 Hz) (means ± SEM) across stimulation conditions, as compared to the stimulation-off condition. RM-ANOVA revealed a significant effect of DBS stimulation condition on tremor ($P < 0.0001$, $n = 4$), and Fisher's PLSD test was used to perform post hoc comparisons between stimulation conditions (*$P < 0.05$). GA and 185-Hz DBS significantly reduced tremor relative to baseline ($P = 0.01$ and $P < 0.0001$, respectively) and relative to 45-Hz DBS ($P = 0.048$ and $P < 0.0001$, respectively). However, 45-Hz DBS did not significantly reduce tremor relative to baseline ($P = 0.45$). Individual colored symbols represent individual participants. (**D**) Changes in TRS (means ± SEM) across stimulation conditions predicted from accelerometer measurements, compared to baseline.

in a stimulation frequency–dependent manner, similar to the frequency-dependent amelioration of clinical motor symptoms (*11*, *24*, *31*, *32*). We recorded field potentials from motor cortex and GP ipsilateral to the dopaminergic lesion and STN stimulating electrodes and quantified suppression of 7- to 10-Hz oscillations in hemiparkinsonian rats during stimulation with each pattern. We observed a significant effect of DBS pattern on 7- to 10-Hz power in both GP and ipsilateral motor cortex. Low-frequency oscillatory power was

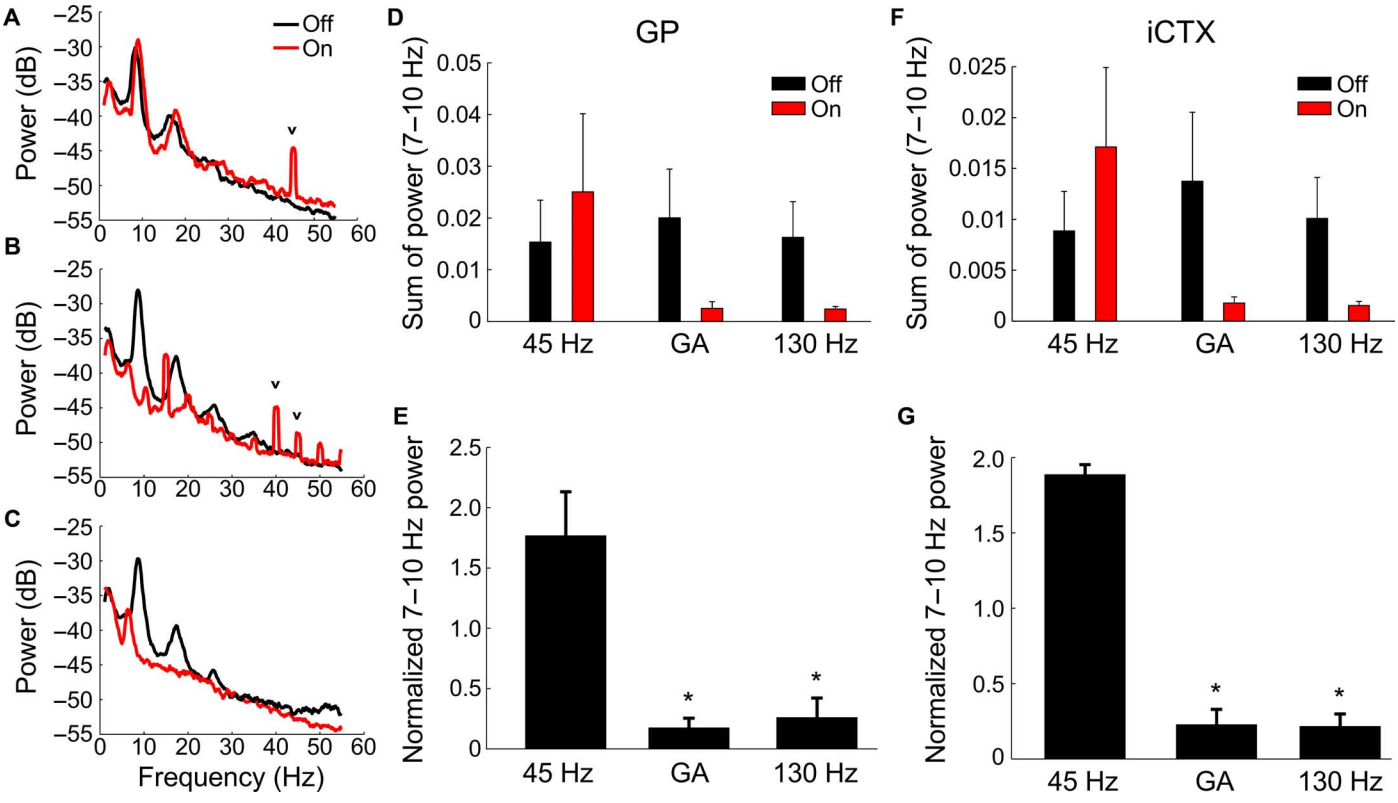

Fig. 5. Effect of temporal pattern of STN DBS on low-frequency oscillations in the GP and ipsilateral cortex of hemiparkinsonian rats. (**A** to **C**) Power spectra of local field potentials recorded from the GP during regular 45-Hz (A), GA (B), and regular 130-Hz DBS (C). The small, narrow peaks (v) in the power spectra are residual artifacts from amplifier blanking and signal interpolation to minimize the contribution of stimulation artifacts to the recorded signals. (**D** and **F**) Sum of 7- to 10-Hz power (means ± SEM) in the three stimulation conditions in GP (D) and ipsilateral cortex (iCTX) (F). Low-frequency (7- to 10-Hz) oscillatory power during each DBS pattern was normalized by the prestimulation and poststimulation power. (**E** and **G**) Normalized 7- to 10-Hz power (means ± SEM) in the three stimulation patterns in GP (E) and iCTX (G). RM-ANOVA revealed a significant effect of DBS condition on normalized 7- to 10-Hz power in GP ($P = 0.0035$; $n = 3$) and iCTX ($P = 0.0003$; $n = 3$), and Fisher's PLSD test was used to perform post hoc comparisons between stimulation conditions (*$P < 0.05$). GA and regular 130-Hz DBS significantly reduced normalized 7- to 10-Hz power compared to regular 45-Hz DBS in GP ($P = 0.0021$ and $P = 0.0026$, respectively) and in iCTX ($P = 0.0002$).

significantly lower during GA and 130 Hz than during 45 Hz in both GP and motor cortex (Fig. 5).

Human subjects with PD exhibit exaggerated β-band oscillations (*30*), and improvements in bradykinesia after dopamine therapy and high-frequency DBS are associated with reductions in this β activity (*33*). We quantified β-band power across stimulation patterns in six human subjects undergoing surgical implantation of the DBS lead in STN for PD. β-Band power was prominent in the DBS-off condition and was suppressed differentially by the stimulation patterns (Fig. 6A). GA and 130 Hz both significantly suppressed β-band power compared to the off condition and 45 Hz (Fig. 6B). β Power from this cohort of DBS implant subjects was correlated with the finger-tapping performance that we measured in the earlier cohort of subjects undergoing motor symptom measurement across DBS conditions (Fig. 6C).

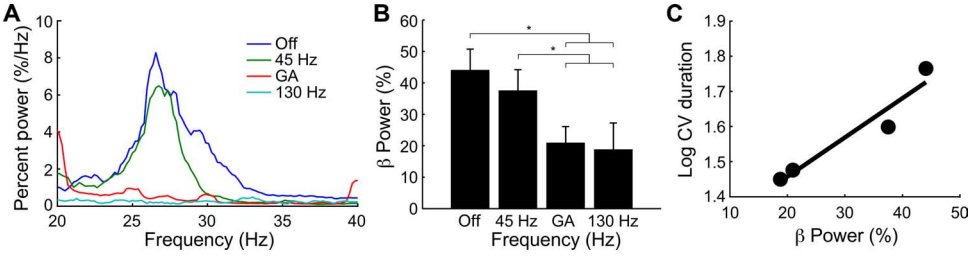

Fig. 6. Effect of temporal pattern of DBS on β-band oscillatory activity in the STN of persons with PD. (**A**) Spectra estimated for the three stimulation conditions. Local field potentials recorded from the STN during DBS lead implant surgery. (**B**) Percent β power quantified across stimulation conditions and averaged across subjects ($n = 6$; means ± SEM). Power in the β range (typically 20 to 33 Hz) was integrated and compared across stimulation conditions. RM-ANOVA revealed a significant effect of DBS condition on percent β power ($P = 0.0007$), and Fisher's PLSD test was used to perform post hoc comparisons between stimulation conditions (*$P < 0.05$). GA DBS and 130-Hz DBS significantly suppressed β power compared to DBS off ($P = 0.0008$ and $P = 0004$, respectively) and 45-Hz DBS ($P = 0.0092$ and $P = 0.0041$, respectively). (**C**) Relationship between percent β power and finger-tapping task performance (as measured by log CV duration). The best-fit line is shown for log CV duration data from Fig. 3C and the percent β power data from (B).

DISCUSSION

We combined model-based optimization using computational evolution, preclinical experiments in a parkinsonian animal model, and

translational experiments in patients with PD to design and evaluate a new temporal pattern of DBS. The optimized temporal pattern achieved efficacy at a low average frequency that was not effective during nonpatterned stimulation. Furthermore, the suppression of low-frequency oscillations by both the GA and high-frequency DBS suggests a potential therapeutic mechanism shared by effective stimulation, whether patterned or unpatterned. Although there is a correlation between β frequency power and bradykinesia (*34*, *35*) and β activity is suppressed by DBS and levodopa (*36*), β activity does not consistently correlate with motor symptoms (*37*), and changes in β activity are inconsistent across patients (*38*, *39*). Therefore, it remains unclear to what degree the suppression of β activity can serve as an index of therapeutic efficacy.

We designed and evaluated a procedure to optimize temporal patterns of neural stimulation to maximize simultaneously efficacy and efficiency. The pattern of DBS emerging from our computational evolution method was only optimal for the specific model and cost function that were used, and it may be possible to improve further the efficacy and efficiency of nonregular patterns of stimulation in a patient-specific manner, for example, by building patient-specific models for optimization.

Our optimized temporal pattern of stimulation that produced symptom relief at a lower average frequency has advantages over conventional high-frequency DBS (typically 130 to 185 Hz). IPGs delivering an optimized low-frequency pattern of stimulation will consume less energy (*12*), and reduced energy consumption translates into longer battery life and less frequent IPG replacement (*13*, *40*). We estimated that the subjects included in this study would achieve an average of 3.9 years of additional battery life had they used GA DBS instead of their current high-frequency DBS (fig. S3). In contrast to previous work with DBS at frequencies less than 100 Hz (*41*), the stimulation pulse width and amplitude in our study were identical to those used for high-frequency stimulation, but the optimized temporal (GA) pattern delivered substantially less electrical energy (*12*). Lower average stimulation frequencies may also decrease stimulation side effects, because there is an inverse relationship between stimulation frequency and side effect intensity (*10*, *11*). However, the nature of the intraoperative testing environment precluded assessment of the effect of stimulation pattern on the side effects produced by DBS. Intermittent DBS may be an alternative approach to reduce stimulation energy, but intermittent thalamic stimulation in patients with essential tremor (*42*, *43*) and intermittent STN DBS in patients with PD (*19*) were less effective than constant stimulation.

The short duration of DBS and assessment of symptoms is a limitation of our studies. Although similar trial lengths are used in studies of parameter settings (*11*, *32*) and for intraoperative testing and postoperative tuning, they may be too short to enable full development of the effects of stimulation. Tremor reduction after onset of DBS and recovery after cessation of DBS occur within seconds (*21*, *44*, *45*), and about 85% of the reduction of bradykinesia occurs within 2 min of starting DBS (*46*). Our short trials may have underestimated the changes in symptoms, but this underestimation would be similar across stimulation patterns and therefore allow valid relative comparisons.

The GA DBS performance was equivalent to high-frequency DBS in the bradykinesia-related finger-tapping task. The predicted changes in UPDRS motor subscores produced by stimulation with the GA pattern were equivalent to those produced by 185 Hz, comparable to those in large, randomized trials of DBS (*47*–*49*), and exceeded the threshold for large clinically important differences (*50*, *51*). This suggests that GA and 185-Hz DBS will provide functionally similar alleviation of motor symptoms and clinically meaningful symptom improvement in bradykinesia-dominant PD patients. The suppression of parkinsonian tremor by GA DBS was somewhat lower than by high-frequency DBS, suggesting that our GA DBS pattern may be most appropriate for patients with mild tremor whose primary symptom is bradykinesia. The differential effect on symptoms was consistent with the relationship between EI, used as a model-based proxy for symptoms during the design process, and bradykinesia observed in previous clinical experiments (*18*) and points to an opportunity for optimizing tremor-specific temporal patterns of stimulation by using a tremor-related outcome measure in the computational model.

One of the desired outcomes from a closed-loop DBS system for PD and other neurological disorders (*16*, *52*, *53*) is energy savings resulting from the demand-controlled stimulation. However, the energy required for feedback signal amplification, acquisition, and processing may mitigate possible energy savings from demand-controlled stimulation. In addition, this approach is currently hindered by difficulty in selecting and recording a symptom-relevant biomarker. Conversely, nonregular temporal patterns of DBS with a low average frequency can provide substantial increases in energy efficiency while bypassing challenges associated with closed-loop systems.

MATERIALS AND METHODS

Study design

The aim of this study was to design an optimized pattern of DBS (GA) and evaluate its efficacy and mechanisms in hemiparkinsonian rats and human subjects with PD. Our hypothesis, based on the computational modeling results, was that GA would reduce motor symptoms in hemiparkinsonian rats and human subjects with PD to the same extent as regular high-frequency stimulation. Rat behavioral experiments were designed on the basis of power analyses that indicated that 10 rats would reveal differences between effective and ineffective stimulation patterns. We projected enrollment numbers of subjects with PD based on a previous study, but as an exploratory proof-of-concept study and acute intervention, we did not have explicit stoppage or end point criteria. The order of stimulation pattern presentation was randomized across all experiments in rats and humans, and predefined quantitative measures of motor performance were used to assess parkinsonian symptoms.

Computation model of the basal ganglia

Temporal patterns of DBS were designed by using a biophysical network model of the basal ganglia and thalamus in the PD state. The model was modified from the original version (*23*) to represent better neural activity and effects of DBS in PD (*54*). The model included 10 neurons in each of the GPe, STN, GPi, and thalamus. The single-compartment model neurons received constant applied currents to represent putative afferent projections that maintained average firing rates, consistent with observations in nonhuman primate models of PD and humans with PD (*55*–*58*). Thalamic neurons did not receive constant applied currents but rather received excitatory pulse inputs intended to represent action potentials from the sensorimotor cortex, which arrived at a frequency of 14 Hz (±20%). EI was calculated by quantifying the fidelity of the thalamic neurons' responses to these inputs. STN DBS was applied by delivering the pattern of current pulses to each STN neuron. Model simulations were

implemented in MATLAB using the forward Euler method with a time step of 0.01 ms and a total simulated time of 50 s.

Stimulation pattern design using a GA

A GA is an optimization technique based on principles from biological evolution (*59*). Patterns of stimulation were encoded using bit strings. Each bit in the string represented 1 ms of time, and the bit's value indicated whether a DBS current pulse was present (1) or not (0) in that epoch. Bit strings contained 200 elements, making each pattern 200 ms long. During initial testing of the GA, we used an iterative empirical process to identify an appropriate pattern length; longer pattern lengths required many more generations to converge, whereas patterns that were too short did not result in optimal solutions. To evaluate the DBS patterns in the model, we applied the 200-ms repeating pattern to the STN neurons. After a random initial population of patterns was generated, patterns were evaluated using a cost function and "mated" to create a new population or generation of patterns. After 90 generations, the optimized pattern of stimulation was selected for testing in hemiparkinsonian rats and patients with PD. The resulting optimal pattern was a repeating vector of interpulse intervals (2, 50, 16, 4, 52, 19, 2, 48, and 7 ms). Multiple iterations of the optimization algorithm yielded highly reproducible temporal patterns.

Each pattern's performance in the computational model was calculated using a cost function,

$$\text{Cost} = 100\%^{*}\frac{\text{EI}_{\text{pattern}} - \text{EI}_{\text{FMC}}}{\text{EI}_{\text{FMC}}}$$

where $\text{EI}_{\text{pattern}}$ was the pattern's EI and EI_{FMC} was the EI of the pattern's frequency-matched regular DBS control pattern. Therefore, the cost function was the percent change in EI compared to the pattern's frequency-matched regular DBS control. Because high-frequency regular DBS was highly effective in the model (*23*, *54*), this cost function incentivized low average frequency patterns of stimulation that suppressed errors in the model without explicitly including stimulation frequency in the cost function.

Several lines of evidence support the use of the thalamic relay EI as a model-based proxy for parkinsonian symptoms. Changes in EI as a function of DBS frequency (*54*) parallel changes in parkinsonian symptoms in 6-OHDA–lesioned rats during different frequencies of STN DBS (*24*). Similarly, there is a strong correlation between the EI in the model and bradykinesia in persons with PD across different random temporal patterns of DBS (*18*). Also, driving the model with GPi activity recorded from parkinsonian nonhuman primates resulted in a high EI, whereas driving the model with GPi activity recorded during therapeutic DBS resulted in a lower EI (*60*). However, these correlations do not necessitate that the EI is a direct measure of motor performance but rather that there is a strong correlation between the effects of DBS on EI and motor symptoms (*60*).

Selective pressure toward more fit patterns was exerted using a roulette wheel parent selection process (*59*) that gave parents with greater fitness a better chance to mate and pass their genes to the next generation. Patterns were numbered from high to low fitness, and parents were selected by iteratively selecting pairs of numbers from an exponential distribution with mean equal to half the population size. One-point crossover was used to exchange genetic material between the parents and to generate two offspring patterns of stimulation as part of the next generation of patterns. After the offspring were generated, 0.1% of their binary string elements were randomly chosen and switched to mimic genetic mutation. Of the 150 patterns in each generation, 130 patterns were children of the previous generation, 10 patterns were randomly generated immigrants incorporated to add genetic diversity and prevent convergence to local minima, and 10 patterns were the most fit patterns from the previous generation included to assure that optimal patterns were maintained in subsequent generations.

Experimental testing in hemiparkinsonian rats

Experiments were conducted in female Long-Evans rats weighing 250 to 350 g. Platinum-iridium stimulation electrode arrays (2 × 2, 10 kilohms, MicroProbe Inc.) were implanted under isoflurane (1 to 3%) anesthesia into the STN using stereotactic technique and acute, single-channel intraoperative recordings to guide placement [A, −3.6 mm; L, 2.6 mm; and V, −6.8 mm, relative to bregma; (*61*)]. Rats were rendered hemiparkinsonian by injection of 6-OHDA into the median forebrain bundle (A, −2.0 mm; L, 2.0 mm; and V, −7.0 mm) via a cannula implanted during the preceding electrode implantation surgery. Desipramine [5 mg/kg intraperitoneally (ip)] and pargyline (50 mg/kg ip) were injected 30 min before 6-OHDA lesion to limit its nonspecific neurotoxic effects (*62*) and to maximize the toxic effects of 6-OHDA on dopaminergic neurons (*63*).

Four STN DBS conditions (off, 45 Hz, 130 Hz, and GA) were evaluated in the hemiparkinsonian rats using two independent, unbiased, and quantitative outcome measures to evaluate the effects of the temporal pattern of DBS: the bar test and methamphetamine-induced circling. DBS at 130 Hz produces maximal reduction of parkinsonian symptoms in rats; however, in contrast to human, increasing the frequency to 185 Hz in rats is more likely to produce side effects including dyskinesia-like movements (*24*, *25*); thus, lower-frequency regular DBS (130 Hz) was used in rats than in humans (185 Hz). All patterns used symmetric, 90 μs per phase biphasic pulses. Stimulation patterns were generated using MATLAB scripts and output through an isolated voltage-to-current convertor (Analog Stimulus Isolator, Model 2200, A-M Systems) and a custom ac coupler.

Bar test

The bar test is a well-established method to quantify akinesia and rigidity in hemiparkinsonian rats (*64*, *65*). Rats were injected with haloperidol—a long-acting, nonspecific dopamine receptor antagonist—and were placed in a clear box containing a bar 10 cm above the floor. The forepaws were placed on the bar, and the amount of time before the rat dismounted from this unnatural position was recorded as a measure of akinesia. Nonlesioned and drug-naive control animals dismounted the bar in 6.4 ± 2.6 s (n = 4; means ± SEM). Haloperidol doses (0.5 to 5.0 mg/kg ip) were titrated for each rat to a dose that resulted in the rat staying on the bar for over 5 min (*24*). Rats were allowed to grip the bar for a maximum of 5 min per trial, and trials started every 10 min after injection. Three trials were performed to confirm the akinetic effect after haloperidol injection, and then 30 min of continuous stimulation was applied, and the time required to dismount the bar was recorded and summed across three trials. Experiments testing the different stimulation patterns were carried out on nonconsecutive days under the same conditions.

Methamphetamine-induced circling

Methamphetamine-induced circling is a well-established method for evaluating locomotor behavior in hemiparkinsonian rats (*66*) and

exhibits DBS frequency-dependent rescue of ipsiversive circling behavior that parallels frequency-dependent suppression of motor symptoms observed in clinical studies (*25*). Methamphetamine (1.25 to 2.5 mg/kg ip) was administered to the rat, and it was placed in a dark cylindrical chamber. An infrared camera and behavioral analysis software (Clever Sys Inc.) recorded and quantified the rat's rotational asymmetry. Stimulation patterns were presented in randomized order within each block. Four to 10 consecutive blocks were run with each rat. Angular velocity and linear speed were quantified for each 1-min epoch of stimulation across patterns and normalized by the angular velocity and linear speed during 1-min epochs just before and after the DBS on condition.

Field potential recordings in rats

We implanted stainless steel screws over motor cortex and microwire electrodes in GP to record field potentials during DBS (n = 3). Platinum-iridium electrode arrays (2 × 2, 10 kilohms, MicroProbe Inc.) were implanted ipsilateral to the STN stimulating electrodes under isoflurane (1 to 3%) anesthesia into the GP using stereotactic technique [A: −1.0 mm; L, 3.0 mm; and V, −5.2 mm, relative to bregma; (*61*)]. Stainless steel screws (1 mm in diameter) were positioned juxtaposed to the dura over ipsilateral motor cortex [A, 2.5 mm and L, 2.5 mm (n = 2) or A, 4.5 mm and L, 2.0 mm (n = 1), relative to bregma; (*61*)]. All recordings of neural activity were referenced to titanium screws inserted through the skull over the cerebellum. After recovering from surgery and from the 6-OHDA lesioning procedure described above, the rats were placed in a Faraday cage, and neural signals were recorded in the freely moving animal. Recordings for each rat took place over the course of 27 min: 9 min for each stimulation condition divided into 3-min prestimulation, 3-min during stimulation, and 3-min poststimulation epochs. Field potential recordings were band-pass–filtered (0.7 to 300 Hz, two and four poles, respectively) and amplified 5000× before digital sampling at 2 kHz (Plexon Multichannel Acquisition Processor System). Multitaper spectral estimates were obtained using the Chronux neural signal analysis package (http://chronux.org) and MATLAB.

Histology

Rats were deeply anesthetized with sodium pentobarbital and sacrificed via intracardiac perfusion with 4% paraformaldehyde. Brains were removed, postfixed, sucrose-protected, and sectioned coronally at a thickness of 50 μm. Tyrosine hydroxylase immunochemistry was used to confirm the effectiveness of unilateral 6-OHDA lesion (fig. S4A). Cresyl violet and cytochrome oxidase staining were used to determine electrode placement, and only rats with stimulating electrodes placed in the STN were included in the analysis (fig. S4B).

Motor symptom evaluation in persons with PD

The Institutional Review Boards at Duke University and Emory University approved the study protocol, and subjects participated on a volunteer basis after providing written informed consent. Inclusion criteria were as follows: at least 3 months after DBS electrode implant, the subject was capable of performing a simple motor evaluation task, neurologically stable, and capable of understanding the study and consent form. Seventeen subjects were consented for the study. Three subjects did not complete the experimental protocol; five subjects failed to exhibit better performance during high-frequency DBS compared to baseline (DBS off) and were excluded from analysis; one subject's data were discarded because of an inability to confirm that stimulation was delivered; and eight subjects completed the protocol and were analyzed. Subjects were asked to withhold PD medications for 12 hours before surgery, and most subjects (six of eight) complied.

Intraoperative stimulation protocol and motor performance measurements

The IPG replacement surgery was performed under local anesthetic (lidocaine). After removal and disconnection of the depleted IPG, a sterile connection was made between the extension cable and the signal generation equipment (*20*, *67*). We quantified motor symptoms unilaterally in subjects with PD—either bradykinesia or tremor—across four conditions: off, 45 Hz, 185 Hz, and GA. Although previous studies indicated no difference in the effects of DBS on tremor, rigidity, or bradykinesia between 130 and 185 Hz (*8*, *11*, *32*), all subjects were programmed to 185 Hz (using their optimal electrode contact pattern) for testing to avoid different control frequencies across subjects. After completion of the motor symptom evaluation task, the sterile connection between the extension cable and the signal generation equipment was disengaged, and the IPG replacement surgery was completed.

Bradykinesia was quantified in bradykinesia-dominant PD subjects using an alternating finger-tapping task (*27*, *68*–*71*), because the time and physical constraints of the intraoperative environment did not allow the use of the UPDRS to assess outcomes. The hand contralateral to stimulation was placed on a two-button computer mouse, and the subject was instructed to press alternately the buttons as regularly and as rapidly as possible during 20-s trials. Trials were repeated three times during each 5-min stimulation-on or stimulation-off epoch, but only the two late trials—starting about 210 or 270 s into the 5-min epoch—were analyzed to account for the time course of the effects of DBS on motor symptoms (*72*, *73*). Analyses including the early trial are included in fig. S5. After the baseline condition, the order of stimulation pattern presentation was randomized, and subjects were blinded to the stimulation conditions. The log-transformed CV of tap duration is more strongly correlated with the UPDRS motor score than tapping rate, particularly with the bradykinesia subscore (*27*) and was used as the outcome measure for bradykinesia across stimulation conditions (*20*). Changes from baseline in log CV duration for each patient were scaled by the gain from the significant correlation between UPDRS part III scores and log CV duration (80 UPDRS motor points per 0.75 log units) to predict stimulation-induced changes in UPDRS motor examination scores across stimulation patterns (*18*, *20*, *27*) and to estimate the clinical impact of the different patterns of stimulation.

Experiments in tremor-dominant PD subjects were performed using an accelerometer taped to the dorsum of the subject's hand and a randomized block design with three blocks and 1-min stimulation-on–stimulation-off pairs. During 20-s trials, the subject was instructed to maintain his or her hand in a fixed position and refrain from voluntary movements. Signals from the three accelerometer axes (x, y, and z) were detrended using a linear regression–based local detrending algorithm (2-s window and 1-s step size), and power spectra were estimated using Welch's method with a 1-s Hanning window and 50% window overlap and summed across all three axes. The peak tremor frequency was between 4 and 5 Hz, and we quantified tremor by integrating the power between 2 and 20 Hz to capture the primary peak and the first three harmonics. The change in log-transformed power between 2 and 20 Hz was calculated for each stimulation off-on pair, averaged across blocks, and used as the outcome measure for tremor across stimulation conditions.

To estimate the clinical impact of different stimulation patterns on tremor, we calculated changes in five-point TRS scores between off-on stimulation pairs using:

$$\Delta\mathrm{TRS} = \frac{1}{\alpha}\log\left(\frac{T_2}{T_1}\right)$$

where T is the tremor amplitude, ΔTRS is the change in TRS score, and α is an empirically derived linear correlation coefficient [α = 0.4, conservatively; (*29*)]. Tremor amplitude is proportional to the square root of the tremor acceleration power. Therefore, we used the square root of the 2- to 20-Hz tremor power (described above) as a proxy for tremor amplitude and calculated the change in TRS score across patterns.

Intraoperative STN field potential recordings in subjects with PD

Field potentials were recorded from the STN in a separate cohort of nine subjects during DBS lead implant surgery rather than during IPG replacement surgery, using instrumentation described elsewhere (*74*). Three additional subjects were consented for the study but withdrew before any intraoperative recordings were performed. All subjects were off medications for PD for at least 12 hours before surgery.

The recording instrumentation consisted of battery-powered low-noise voltage preamplifiers (SR560, Stanford Research Systems) with amplifier blanking in a serial configuration with diode clamps between stages (*74*). The relay at the stimulator that disconnected the stimulating contact between pulses, as described in (*74*), was removed, and the amplifiers were blanked between 20 μs before through 20 to 500 after each DBS pulse, which allowed sufficient gain (2000× to 10,000×) for field potential recordings without saturation. Although the stimulation waveforms and patterns were the same across all subjects, the duration of stimulation artifacts was variable, apparently as a result of differences in the tissue properties around the electrodes (*75*). Therefore, the amplifier blanking duration was tuned individually for each patient.

Symmetric biphasic pulses (90 μs per phase) were delivered through contact 1 or 2 on the DBS electrode lead (whichever was determined to be clinically effective by the attending neurologist), and the stimulation counter electrode was placed on the chest (StimCare Carbon Foam Electrode, Empi). Bipolar recordings were made from contacts 0 and 2 ($0^+/2^-$) or contacts 1 and 3 ($1^+/3^-$) on the DBS electrode lead, and the implanted cannula served as the recording reference electrode. The four-contact lead is implanted to place at least two contacts (typically 1 and 2 but occasionally 0 and 1) within the T2-positive region considered to be STN on magnetic resonance imaging (fusing the postoperative CT scan with the preoperative magnetic resonance imaging scan), and electrode tracks were located within the STN with >4-mm electrode track depth of STN. Stimulation was delivered at an amplitude determined to be effective by the neurologist performing the intraoperative assessment (1.5 to 3.0 V). GA, 45 Hz, and 130 Hz were presented in randomized order for 60-s (n = 4) or 300-s (n = 5) intervals with intervening intervals of no stimulation. One subject received only 130 Hz before withdrawing and was excluded from analysis.

Our objective was to quantify the effects of DBS on ongoing β-band activity, because previous data suggested that this activity is correlated with bradykinesia in PD (*34*, *35*) and changes in response to DBS in a manner that paralleled the changes in symptoms (*36*). The field potential data were high-pass–filtered to remove offset and very slow signal components (2-Hz cutoff, three-pole Butterworth filter, and MATLAB), and the signal was smoothed around the amplifier blanking epoch by linear interpolation from 0.1 ms before to 1.5 ms after the start of the DBS pulse. Evoked compound action potentials were observed in the interpulse intervals (*75*), and the averaged evoked response was subtracted from the signal to reduce spectral power at the stimulation frequency. Finally, the data were band-pass–filtered between 2 and 100 Hz and downsampled to 400 Hz before spectral analysis (http://chronux.org). The final 20 or 95 s of data from the 60- and 300-s trials for each condition was selected for spectral analysis (except in one subject who did not complete 300 s of data collection for 130 Hz, and a 15-s trial was used in its place). β Power was quantified as the percentage of power in a 14-Hz window centered around the β peak in the off condition. Two subjects were excluded from analysis because they did not have a prominent β peak in the off condition (defined as <1%/Hz peak power in a β band), leaving six subjects included in the analysis. In most subjects, this window coincided well with the high β range (20 to 33 Hz). However, in one subject, the β peak was at 14 Hz, and the window was contracted so that it did not include frequencies below 10 Hz.

The data processing methods did not artificially reduce β power in the recorded field potentials for the GA condition. The two subjects who did not have β peaks in their field potential spectra had increased β power due to the GA pattern data processing methods, which introduced small spectral artifacts in the β range (fig. S6).

Statistical analysis

Finger-tapping and tremor data were collected using LabVIEW and were processed in MATLAB. Technical outliers were removed from the mouse clicking data by discarding extremely short clicks that were artifacts of the computer mouse clicking apparatus (debouncing; visual inspection of click duration histograms; fig. S7). Statistical analyses were conducted in StatView 5.0.1 for Windows. All rat and human data were analyzed using repeated-measures ANOVA. Post hoc comparisons between stimulation patterns were performed when indicated by repeated-measures ANOVA using the Fisher's protected least significant difference test with significance defined at α = 0.05.

SUPPLEMENTARY MATERIALS

www.sciencetranslationalmedicine.org/cgi/content/full/9/371/eaah3532/DC1

Fig. S1. Effect of stimulation pattern on total distance traveled during the methamphetamine-induced circling task.

Fig. S2. Effects of stimulation patterns on finger-tapping rates in persons with PD and STN DBS.

Fig. S3. Estimated battery longevity by subject with GA DBS compared to their clinical parameters.

Fig. S4. Examples of postmortem histology.

Fig. S5. Finger-tapping log CV duration for all three finger-tapping trials in each 5-min epoch.

Fig. S6. Example data from a subject who did not exhibit a β peak in the spectrum of field potentials recorded in STN.

Fig. S7. Histograms of tap duration for each subject in the finger-tapping task.

Table S1. Individual subject-level data.

REFERENCES AND NOTES

1. D. J. Gelb, E. Oliver, S. Gilman, Diagnostic criteria for Parkinson disease. *Arch. Neurol.* **56**, 33–39 (1999).
2. A. J. Hughes, S. E. Daniel, L. Kilford, A. J. Lees, Accuracy of clinical diagnosis of idiopathic Parkinson's disease: A clinico-pathological study of 100 cases. *J. Neurol. Neurosurg. Psychiatry* **55**, 181–184 (1992).

3. R. P. Lesser, S. Fahn, S. R. Snider, L. J. Cote, W. P. Isgreen, R. E. Barrett, Analysis of the clinical problems in parkinsonism and the complications of long-term levodopa therapy. *Neurology* **29**, 1253–1260 (1979).
4. A. L. Benabid, S. Chabardes, J. Mitrofanis, P. Pollak, Deep brain stimulation of the subthalamic nucleus for the treatment of Parkinson's disease. *Lancet Neurol.* **8**, 67–81 (2009).
5. E. Moro, A. M. Lozano, P. Pollak, Y. Agid, S. Rehncrona, J. Volkmann, J. Kulisevsky, J. A. Obeso, A. Albanese, M. I. Hariz, N. P. Quinn, J. D. Speelman, A. L. Benabid, V. Fraix, A. Mendes, M.-L. Welter, J.-L. Houeto, P. Cornu, D. Dormont, A. L. Tornqvist, R. Ekberg, A. Schnitzler, L. Timmermann, L. Wojtecki, A. Gironell, M. C. Rodriguez-Oroz, J. Guridi, A. R. Bentivoglio, M. F. Contarino, L. Romito, M. Scerrati, M. Janssens, A. E. Lang, Long-term results of a multicenter study on subthalamic and pallidal stimulation in Parkinson's disease. *Mov. Disord.* **25**, 578–586 (2010).
6. F. M. Weaver, K. Follett, M. Stern, K. Hur, C. Harris, W. J. Marks Jr., J. Rothlind, O. Sagher, D. Reda, C. S. Moy, Bilateral deep brain stimulation vs best medical therapy for patients with advanced Parkinson disease. *JAMA* **301**, 63–73 (2009).
7. A. L. Benabid, P. Pollak, C. Gross, D. Hoffmann, A. Benazzouz, D. M. Gao, A. Laurent, M. Gentil, J. Perret, Acute and long-term effects of subthalamic nucleus stimulation in Parkinson's disease. *Stereotact. Funct. Neurosurg.* **62**, 76–84 (1994).
8. P. Limousin, P. Pollak, A. Benazzouz, D. Hoffmann, J. F. Le Bas, E. Broussolle, J. E. Perret, A. L. Benabid, Effect on parkinsonian signs and symptoms of bilateral subthalamic nucleus stimulation. *Lancet* **345**, 91–95 (1995).
9. J. Siegfried, B. Lippitz, Bilateral chronic electrostimulation of ventroposterolateral pallidum: A new therapeutic approach for alleviating all parkinsonian symptoms. *Neurosurgery* **35**, 1126–1129 (1994).
10. A. M. Kuncel, S. E. Cooper, B. R. Wolgamuth, M. A. Clyde, S. A. Snyder, E. B. Montgomery Jr., A. R. Rezai, W. M. Grill, Clinical response to varying the stimulus parameters in deep brain stimulation for essential tremor. *Mov. Disord.* **21**, 1920–1928 (2006).
11. M. Rizzone, M. Lanotte, B. Bergamasco, A. Tavella, E. Torre, G. Faccani, A. Melcarne, L. Lopiano, Deep brain stimulation of the subthalamic nucleus in Parkinson's disease: Effects of variation in stimulation parameters. *J. Neurol. Neurosurg. Psychiatry* **71**, 215–219 (2001).
12. A. M. Koss, R. L. Alterman, M. Tagliati, J. L. Shils, Calculating total electrical energy delivered by deep brain stimulation systems. *Ann. Neurol.* **58**, 168 (2005).
13. M. Bin-Mahfoodh, C. Hamani, E. Sime, A. M. Lozano, Longevity of batteries in internal pulse generators used for deep brain stimulation. *Stereotact. Funct. Neurosurg.* **80**, 56–60 (2003).
14. J. Pepper, L. Zrinzo, B. Mirza, T. Foltynie, P. Limousin, M. Hariz, The risk of hardware infection in deep brain stimulation surgery is greater at impulse generator replacement than at the primary procedure. *Stereotact. Funct. Neurosurg.* **91**, 56–65 (2013).
15. K. B. Baker, J. Zhang, J. L. Vitek, Pallidal stimulation: Effect of pattern and rate on bradykinesia in the non-human primate model of Parkinson's disease. *Exp. Neurol.* **231**, 309–313 (2011).
16. B. Rosin, M. Slovik, R. Mitelman, M. Rivlin-Etzion, S. N. Haber, Z. Israel, E. Vaadia, H. Bergman, Closed-loop deep brain stimulation is superior in ameliorating parkinsonism. *Neuron* **72**, 370–384 (2011).
17. G. C. McConnell, R. Q. So, W. M. Grill, Failure to suppress low-frequency neuronal oscillatory activity underlies the reduced effectiveness of random patterns of deep brain stimulation. *J. Neurophysiol.* **115**, 2791–2802 (2016).
18. A. D. Dorval, A. M. Kuncel, M. J. Birdno, D. A. Turner, W. M. Grill, Deep brain stimulation alleviates parkinsonian bradykinesia by regularizing pallidal activity. *J. Neurophysiol.* **104**, 911–921 (2010).
19. E. Montgomery Jr., Effect of subthalamic nucleus stimulation patterns on motor performance in Parkinson's disease. *Parkinsonism Relat. Disord.* **11**, 167–171 (2005).
20. D. T. Brocker, B. D. Swan, D. A. Turner, R. E. Gross, S. B. Tatter, M. M. Koop, H. Bronte-Stewart, W. M. Grill, Improved efficacy of temporally non-regular deep brain stimulation in Parkinson's disease. *Exp. Neurol.* **239**, 60–67 (2013).
21. M. J. Birdno, A. M. Kuncel, A. D. Dorval, D. A. Turner, W. M. Grill, Tremor varies as a function of the temporal regularity of deep brain stimulation. *Neuroreport* **19**, 599–602 (2008).
22. M. J. Birdno, A. M. Kuncel, A. D. Dorval, D. A. Turner, R. E. Gross, W. M. Grill, Stimulus features underlying reduced tremor suppression with temporally patterned deep brain stimulation. *J. Neurophysiol.* **107**, 364–383 (2012).
23. J. E. Rubin, D. Terman, High frequency stimulation of the subthalamic nucleus eliminates pathological thalamic rhythmicity in a computational model. *J. Comput. Neurosci.* **16**, 211–235 (2004).
24. G. C. McConnell, R. Q. So, J. D. Hilliard, P. Lopomo, W. M. Grill, Effective deep brain stimulation suppresses low-frequency network oscillations in the basal ganglia by regularizing neural firing patterns. *J. Neurosci.* **32**, 15657–15668 (2012).
25. R. Q. So, G. C. McConnell, A. T. August, W. M. Grill, Characterizing effects of subthalamic nucleus deep brain stimulation on methamphetamine-induced circling behavior in hemi-parkinsonian rats. *IEEE Trans. Neural Syst. Rehabil. Eng.* **20**, 626–635 (2012).
26. Q. Li, Y. Ke, D. C. W. Chan, Z.-M. Qian, K. K. L. Yung, H. Ko, G. W. Arbuthnott, W.-H. Yung, Therapeutic deep brain stimulation in Parkinsonian rats directly influences motor cortex. *Neuron* **76**, 1030–1041 (2012).
27. A. L. Taylor Tavares, G. S. X. E. Jefferis, M. Koop, B. C. Hill, T. Hastie, G. Heit, H. M. Bronte-Stewart, Quantitative measurements of alternating finger tapping in Parkinson's disease correlate with UPDRS motor disability and reveal the improvement in fine motor control from medication and deep brain stimulation. *Mov. Disord.* **20**, 1286–1298 (2005).
28. C. Hamani, E. Richter, J. M. Schwalb, A. M. Lozano, Bilateral subthalamic nucleus stimulation for Parkinson's disease: A systematic review of the clinical literature. *Neurosurgery* **56**, 1313–1324 (2005).
29. R. J. Elble, S. L. Pullman, J. Y. Matsumoto, J. Raethjen, G. Deuschl, R. Tintner, Tremor amplitude is logarithmically related to 4- and 5-point tremor rating scales. *Brain* **129**, 2660–2666 (2006).
30. P. Brown, Abnormal oscillatory synchronisation in the motor system leads to impaired movement. *Curr. Opin. Neurobiol.* **17**, 656–664 (2007).
31. N. Fogelson, A. A. Kuhn, P. Silberstein, P. D. Limousin, M. Hariz, T. Trottenberg, A. Kupsch, P. Brown, Frequency dependent effects of subthalamic nucleus stimulation in Parkinson's disease. *Neurosci. Lett.* **382**, 5–9 (2005).
32. E. Moro, R. J. A. Esselink, J. Xie, M. Hommel, A. L. Benabid, P. Pollak, The impact on Parkinson's disease of electrical parameter settings in STN stimulation. *Neurology* **59**, 706–713 (2002).
33. N. J. Ray, N. Jenkinson, S. Wang, P. Holland, J. S. Brittain, C. Joint, J. F. Stein, T. Aziz, Local field potential beta activity in the subthalamic nucleus of patients with Parkinson's disease is associated with improvements in bradykinesia after dopamine and deep brain stimulation. *Exp. Neurol.* **213**, 108–113 (2008).
34. A. A. Kühn, A. Kupsch, G.-H. Schneider, P. Brown Reduction in subthalamic 8–35 Hz oscillatory activity correlates with clinical improvement in Parkinson's disease. *Eur. J. Neurosci.* **23**, 1956–1960 (2006).
35. A. Pogosyan, F. Yoshida, C. C. Chen, I. Martinez-Torres, T. Foltynie, P. Limousin, L. Zrinzo, M. I. Hariz, P. Brown, Parkinsonian impairment correlates with spatially extensive subthalamic oscillatory synchronization. *Neuroscience* **171**, 245–257 (2010).
36. A. Eusebio, H. Cagnan, P. Brown Does suppression of oscillatory synchronisation mediate some of the therapeutic effects of DBS in patients with Parkinson's disease. *Front. Integr. Neurosci.* **6**, 47 (2012).
37. M. Weinberger, N. Mahant, W. D. Hutchison, A. M. Lozano, E. Moro, M. Hodaie, A. E. Lang, J. O. Dostrovsky, Beta oscillatory activity in the subthalamic nucleus and its relation to dopaminergic response in Parkinson's disease. *J. Neurophysiol.* **96**, 3248–3256 (2006).
38. M. Rosa, G. Giannicola, D. Servello, S. Marceglia, C. Pacchetti, M. Porta, M. Sassi, E. Scelzo, S. Barbieri, A. Priori, Subthalamic local field beta oscillations during ongoing deep brain stimulation in Parkinson's disease in hyperacute and chronic phases. *Neurosignals* **19**, 151–162 (2011).
39. A. Priori, G. Foffani, L. Rossi, S. Marceglia, Adaptive deep brain stimulation (aDBS) controlled by local field potential oscillations. *Exp. Neurol.* **245**, 77–86 (2013).
40. W. G. Ondo, C. Meilak, K. D. Vuong, Predictors of battery life for the Activa® Soletra 7426 Neurostimulator. *Parkinsonism Relat. Disord.* **13**, 240–242 (2007).
41. E. W. Tsang, C. Hamani, E. Moro, F. Mazzella, U. Saha, A. M. Lozano, M. Hodaie, R. Chuang, T. Steeves, S. Y. Lim, B. Neagu, R. Chen, Subthalamic deep brain stimulation at individualized frequencies for Parkinson disease. *Neurology* **78**, 1930–1938 (2012).
42. A. M. Kuncel, M. J. Birdno, B. D. Swan, W. M. Grill, Tremor reduction and modeled neural activity during cycling thalamic deep brain stimulation. *Clin. Neurophysiol.* **123**, 1044–1052 (2012).
43. B. D. Swan, D. T. Brocker, J. D. Hilliard, S. B. Tatter, R. E. Gross, D. A. Turner, W. M. Grill, Short pauses in thalamic deep brain stimulation promote tremor and neuronal bursting. *Clin. Neurophysiol.* **127**, 1551–1559 (2016).
44. J. Volkmann, J. Herzog, F. Kopper, G. Deuschl, Introduction to the programming of deep brain stimulators. *Mov. Disord.* **17**, S181–S187 (2002).
45. A. Beuter, M. S. Titcombe, Modulation of tremor amplitude during deep brain stimulation at different frequencies. *Brain Cogn.* **53**, 190–192 (2003).
46. L. Lopiano, E. Torre, F. Benedetti, B. Bergamasco, P. Perozzo, A. Pollo, M. Rizzone, A. Tavella, M. Lanotte, Temporal changes in movement time during the switch of the stimulators in Parkinson's disease patients treated by subthalamic nucleus stimulation. *Eur. Neurol.* **50**, 94–99 (2003).
47. P. Krack, A. Batir, N. Van Blercom, S. Chabardes, V. Fraix, C. Ardouin, A. Koudsie, P. D. Limousin, A. Benazzouz, J. F. LeBas, A.-L. Benabid, P. Pollak, Five-year follow-up of bilateral stimulation of the subthalamic nucleus in advanced Parkinson's disease. *N. Engl. J. Med.* **349**, 1925–1934 (2003).
48. G. Deuschl, C. Schade-Brittinger, P. Krack, J. Volkmann, H. Schäfer, K. Bötzel, C. Daniels, A. Deutschländer, U. Dillmann, W. Eisner, D. Gruber, W. Hamel, J. Herzog, R. Hilker, S. Klebe, M. Kloss, J. Koy, M. Krause, A. Kupsch, D. Lorenz, S. Lorenzl, H. M. Mehdorn, J. R. Moringlane, W. Oertel, M. O. Pinsker, H. Reichmann, A. Reuss, G.-H. Schneider, A. Schnitzler, U. Steude, V. Sturm, L. Timmermann, V. Tronnier, T. Trottenberg, L. Wojtecki,

E. Wolf, W. Poewe, J. Voges; German Parkinson Study Group, Neurostimulation Section, A randomized trial of deep-brain stimulation for Parkinson's disease. *N. Engl. J. Med.* **355**, 896–908 (2006).
49. K. A. Follett, F. M. Weaver, M. Stern, K. Hur, C. L. Harris, P. Luo, W. J. Marks Jr., J. Rothlind, O. Sagher, C. Moy, R. Pahwa, K. Burchiel, P. Hogarth, E. C. Lai, J. E. Duda, K. Holloway, A. Samii, S. Horn, J. M. Bronstein, G. Stoner, P. A. Starr, R. Simpson, G. Baltuch, A. De Salles, G. D. Huang, D. J. Reda; CSP 468 Study Group, Pallidal versus subthalamic deep-brain stimulation for Parkinson's disease. *N. Engl. J. Med.* **362**, 2077–2091 (2010).
50. A. Schrag, C. Sampaio, N. Counsell, W. Poewe, Minimal clinically important change on the unified Parkinson's disease rating scale. *Mov. Disord.* **21**, 1200–1207 (2006).
51. L. M. Shulman, A. L. Gruber-Baldini, K. E. Anderson, P. S. Fishman, S. G. Reich, W. J. Weiner, The clinically important difference on the unified Parkinson's disease rating scale. *Arch. Neurol.* **67**, 64–70 (2010).
52. S. Santaniello, G. Fiengo, L. Glielmo, W. M. Grill, Closed-loop control of deep brain stimulation: A simulation study. *IEEE Trans. Neural Syst. Rehabil. Eng.* **19**, 15–24 (2011).
53. S. Stanslaski, P. Afshar, P. Cong, J. Giftakis, P. Stypulkowski, D. Carlson, D. Linde, D. Ullestad, A. T. Avestruz, T. Denison, Design and validation of a fully implantable, chronic, closed-loop neuromodulation device with concurrent sensing and stimulation. *IEEE Trans. Neural Syst. Rehabil. Eng.* **20**, 410–421 (2012).
54. R. Q. So, A. R. Kent, W. M. Grill, Relative contributions of local cell and passing fiber activation and silencing to changes in thalamic fidelity during deep brain stimulation and lesioning: A computational modeling study. *J. Comput. Neurosci.* **32**, 499–519 (2012).
55. H. Bergman, T. Wichmann, B. Karmon, M. R. DeLong, The primate subthalamic nucleus. II. Neuronal activity in the MPTP model of parkinsonism. *J. Neurophysiol.* **72**, 507–520 (1994).
56. P. A. Starr, G. M. Rau, V. Davis, W. J. Marks Jr., J. L. Ostrem, D. Simmons, N. Lindsey, R. S. Turner, Spontaneous pallidal neuronal activity in human dystonia: Comparison with Parkinson's disease and normal macaque. *J. Neurophysiol.* **93**, 3165–3176 (2005).
57. F. Steigerwald, M. Pötter, J. Herzog, M. Pinsker, F. Kopper, H. Mehdorn, G. Deuschl, J. Volkmann, Neuronal activity of the human subthalamic nucleus in the parkinsonian and nonparkinsonian state. *J. Neurophysiol.* **100**, 2515–2524 (2008).
58. T. Wichmann, J. Soares, Neuronal firing before and after burst discharges in the monkey basal ganglia is predictably patterned in the normal state and altered in parkinsonism. *J. Neurophysiol.* **95**, 2120–2133 (2006).
59. L. Davis, *Handbook of genetic algorithms*, L. Davis, Ed. (Van Nostrand Reinhold, 1991).
60. Y. Guo, J. E. Rubin, C. C. McIntyre, J. L. Vitek, D. Terman, Thalamocortical relay fidelity varies across subthalamic nucleus deep brain stimulation protocols in a data-driven computational model. *J. Neurophysiol.* **99**, 1477–1492 (2008).
61. G. Paxinos, C. Watson, *The Rat Brain in Stereotaxic Coordinates: Hard Cover Edition* (Academic Press, ed. 6, 2007).
62. M. T. Lin, T. Y. Kao, C. Chio, Y. T. Jin, Dopamine depletion protects striatal neurons from heatstroke-induced ischemia and cell death in rats. *Am. J. Physiol.* **269**, H487–H490 (1995).
63. R. K. W. Schwarting, J. P. Huston, Unilateral 6-hydroxydopamine lesions of meso-striatal dopamine neurons and their physiological sequelae. *Prog. Neurobiol.* **49**, 215–266 (1996).
64. R. Duvoisin, Parkinsonism: Animal analogues of the human disorder. *Res. Publ. Assoc. Res. Nerv. Ment. Dis.* **55**, 293–303 (1976).
65. P. R. Sanberg, M. D. Bunsey, M. Giordano, A. B. Norman, The catalepsy test: Its ups and downs. *Behav. Neurosci.* **102**, 748–759 (1988).
66. U. Ungerstedt, G. W. Arbuthnott, Quantitative recording of rotational behavior in rats after 6-hydroxy-dopamine lesions of the nigrostriatal dopamine system. *Brain Res.* **24**, 485–493 (1970).
67. B. D. Swan, W. M. Grill, D. A. Turner, Investigation of deep brain stimulation mechanisms during implantable pulse generator replacement surgery. *Neuromodulation* **17**, 419–424 (2014).
68. B. D. Burns, J. D. DeJong, A preliminary report on the measurement of Parkinson's disease. *Neurology* **10**, 1096–1102 (1960).
69. G. Giovannoni, J. van Schalkwyk, V. U. Fritz, A. J. Lees, Bradykinesia akinesia inco-ordination test (BRAIN TEST): An objective computerised assessment of upper limb motor function. *J. Neurol. Neurosurg. Psychiatry* **67**, 624–629 (1999).
70. C. N. Homann, K. Suppan, K. Wenzel, G. Giovannoni, G. Ivanic, S. Horner, E. Ott, H. P. Hartung, The bradykinesia akinesia incoordination test (BRAIN TEST), an objective and user-friendly means to evaluate patients with Parkinsonism. *Mov. Disord.* **15**, 641–647 (2000).
71. P. K. Pal, C. S. Lee, A. Samii, M. Schulzer, A. J. Stoessl, E. K. Mak, J. Wudel, T. Dobko, J. K. C. Tsui, Alternating two finger tapping with contralateral activation is an objective measure of clinical severity in Parkinson's disease and correlates with PET. *Parkinsonism Relat. Disord.* **7**, 305–309 (2001).
72. P. Temperli, J. Ghika, J.-G. Villemure, P. R. Burkhard, J. Bogousslavsky, F. J. G. Vingerhoets, How do parkinsonian signs return after discontinuation of subthalamic DBS? *Neurology* **60**, 78–81 (2003).
73. B. Waldau, D. A. Clayton, L. B. Gasperson, D. A. Turner, Analysis of the time course of the effect of subthalamic nucleus stimulation upon hand function in Parkinson's patients. *Stereotact. Funct. Neurosurg.* **89**, 48–55 (2011).
74. A. R. Kent, W. M. Grill, Recording evoked potentials during deep brain stimulation: Development and validation of instrumentation to suppress the stimulus artefact. *J. Neural Eng.* **9**, 036004 (2012).
75. A. R. Kent, B. D. Swan, D. T. Brocker, D. A. Turner, R. E. Gross, W. M. Grill, Measurement of evoked potentials during thalamic deep brain stimulation. *Brain Stimul.* **8**, 42–56 (2014).

Acknowledgments: We thank G. Mills for laboratory support and A. August for assistance with histology. **Funding:** This work was supported by NIH grants R01 NS040894, R37 NS040894, and R01 NS079312. **Author contributions:** D.T.B. and W.M.G. designed the research; D.T.B., B.D.S., R.Q.S., D.A.T., R.E.G., and W.M.G. performed the research; and D.T.B. and W.M.G. analyzed data and wrote the paper. **Competing interests:** D.T.B. and W.M.G. are inventors on awarded and pending patents related to nonregular patterns of DBS. These patents are owned by Duke University and licensed to Deep Brain Innovations LLC (DBI). W.M.G. is cofounder, director, and chief scientific officer of DBI; both W.M.G. and D.T.B. own equity in DBI. W.M.G. is director and chief scientific officer of NDI Healthcare Fund and NDI Medical LLC, which are investors in DBI, and receives compensation for these positions. These relationships are reported to the Conflict of Interest Committee at Duke University. R.E.G. receives research funding from Medtronic. R.E.G. serves as a consultant to Medtronic, St. Jude Medical, and DBI and receives compensation for these services. The terms of this arrangement have been reviewed and approved by Emory University in accordance with its conflict-of-interest policies. **Data and materials availability:** Experimental results in individual animals and human subjects are provided in the Supplementary Materials.

Submitted 7 December 2015
Resubmitted 15 June 2016
Accepted 18 November 2016
Published 4 January 2017
10.1126/scitranslmed.aah3532

Citation: D. T. Brocker, B. D. Swan, R. Q. So, D. A. Turner, R. E. Gross, W. M. Grill, Optimized temporal pattern of brain stimulation designed by computational evolution. *Sci. Transl. Med.* **9**, eaah3532 (2017).

Science Translational Medicine AAAS

Optimized temporal pattern of brain stimulation designed by computational evolution

David T. Brocker, Brandon D. Swan, Rosa Q. So, Dennis A. Turner, Robert E. Gross and Warren M. Grill (January 4, 2017)

Science Translational Medicine **9** (371), . [doi: 10.1126/scitranslmed.aah3532]

Editor's Summary

Building better DBS with evolution

In deep brain stimulation (DBS), electrodes inserted deep within a patients' brain deliver electric pulses that can alleviate symptoms of Parkinson's disease or tremor or even of diseases such as obsessive-compulsive disorder. Yet, the stimuli are usually standard, with uniform frequencies and amplitudes. To design better stimuli, Brocker *et al*. built a model of Parkinson's disease and used computational evolution to find a new temporal stimulation pattern. Application of this evolution-derived stimulation pattern in animal models and Parkinson's disease patients verified that it was just as effective as the standard stimulation pattern but required significantly less overall energy. Because one drawback of DBS is the need for frequent risky surgeries to change the power source, less drain on the battery means healthier patients.

Science Translational Medicine (print ISSN 1946-6234; online ISSN 1946-6242) is published weekly, except the last week in December, by the American Association for the Advancement of Science, 1200 New York Avenue, NW, Washington, DC 20005.